Supporting Information for "Tropical Anvil Clouds: Radiative Driving Towards a Preferred State"

Adam B. Sokol[1], Dennis L. Hartmann[1]

[1]Department of Atmospheric Sciences, University of Washington, Seattle, WA, USA

Contents of this file

1. Text S1

2. Figures S1 to S7

Introduction

This supporting information includes a brief discussion of the relationship between cloud ice water path (IWP) and optical thickness (τ) in DARDAR-CLOUD v2.1.1. Figures S1-S3 accompany that discussion. Figures S4-S7 provide information referenced in the main text.

The figures in this document are based on cloud retrievals that have been corrected for the diurnal bias in lidar sensitivity (described in section 2.1.2 of the main text).

August 27, 2020, 9:57pm

S1. Relationship between IWP and τ

Here we show that the peak in the anvil cloud τ distribution at $\sim$1.4 (Fig. 4 in the main text) is not an artifact of the IWP threshold used to identify anvil clouds (10 g m^{-2}). Figure S1 shows a joint histogram of IWP and τ for cloud layers in the study region with tops above 10 km. It demonstrates the tight relationship between IWP and τ in DARDAR-CLOUD and reveals that layers with an IWP near the threshold of 10 g m^{-2} (dashed red line) typically have τ between 0.4 and 0.7. Figure S2 shows the median IWP for cloud layers as a function of τ, with shading between the 5th and 95th IWP percentiles. It is clear that cloud layers with τ between 1 and 2 have IWP well in excess of 10 g m^{-2}. The highest τ at which the blue shading spans the IWP threshold (dashed red line) is $\sim$0.75. The anvil τ distribution would therefore be expected to show artificially low frequency for $\tau < 0.75$, but should be largely unaffected at higher τ.

To ensure that the τ distribution in the range of interest is unaffected by the IWP threshold, we test two lower thresholds: 1 and 5 g m^{-2}. These two values belong to the lowest IWP mode of the climatological IWP distribution (Figure 1 in the main text), which we have supposed represents thin cirrus that are not necessarily of convective origin. Nevertheless, we proceed with "anvil" cloud layer identification using the different IWP thresholds and the cloud top and base height criteria described in section 2.1.3 of the main text. The resulting τ distributions, shown in Figure S3, all have a peak at $\sim$1.4 and are nearly identical for $\tau > 0.75$. This provides confidence that the distribution peak is not an artifact of the IWP threshold used for anvil cloud identification.
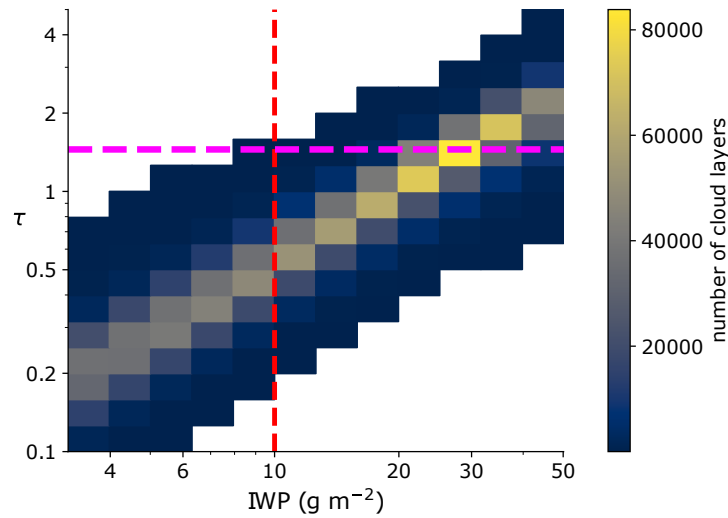
Figure S1. Joint histogram of IWP and τ for cloud layers with tops above 10 km. Dashed red line: IWP threshold used for anvil identification (10 g m^{-2}). Dashed pink line: approximate peak in the anvil τ distribution at 1.4. Bin widths are 0.1 in log space for both IWP and τ. Data are from both the West Pacific and Indian Ocean regions.
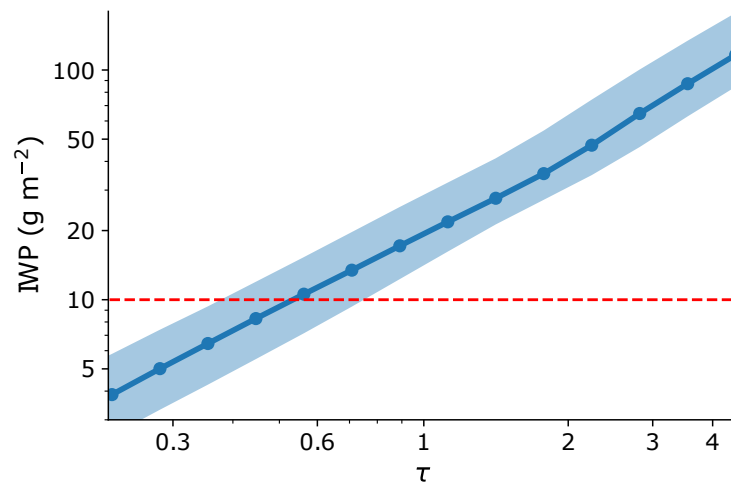

Figure S2. Median IWP as a function of τ for cloud layers with tops above 10 km. Shading is between the 5th and 95th IWP percentiles. Dashed red line: IWP threshold used for anvil identification (10 g m^{-2}). Data are from both the West Pacific and Indian Ocean regions.
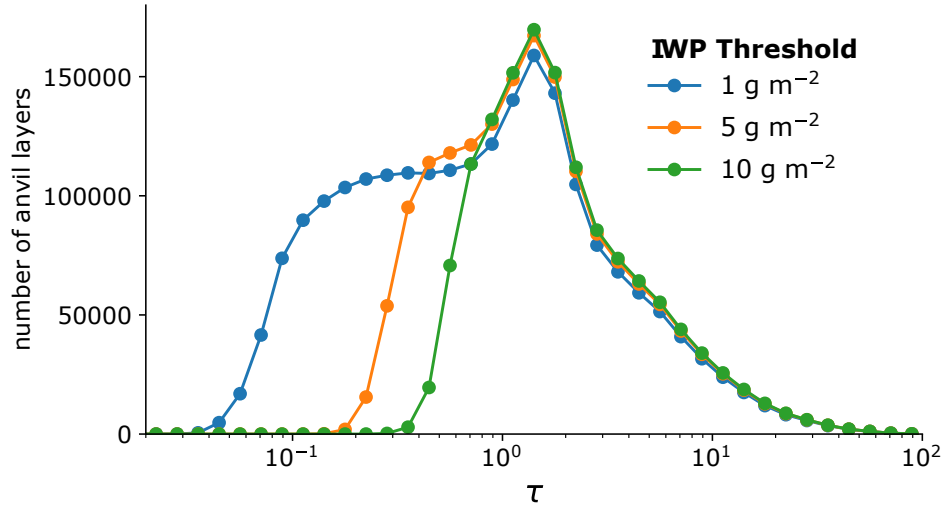
August 27, 2020, 9:57pm

:

Figure S3. Distributions of anvil τ for different IWP thresholds used for anvil identification. The minor differences in the distributions for $\tau1$ result from the disqualification of anvil layers located beneath other anvil layers. When the IWP threshold is lowered, some layers that had previously failed to meet the IWP threshold are newly classified as anvil clouds, which disqualifies any anvil layers located below. Data are from both the West Pacific and Indian Ocean regions.
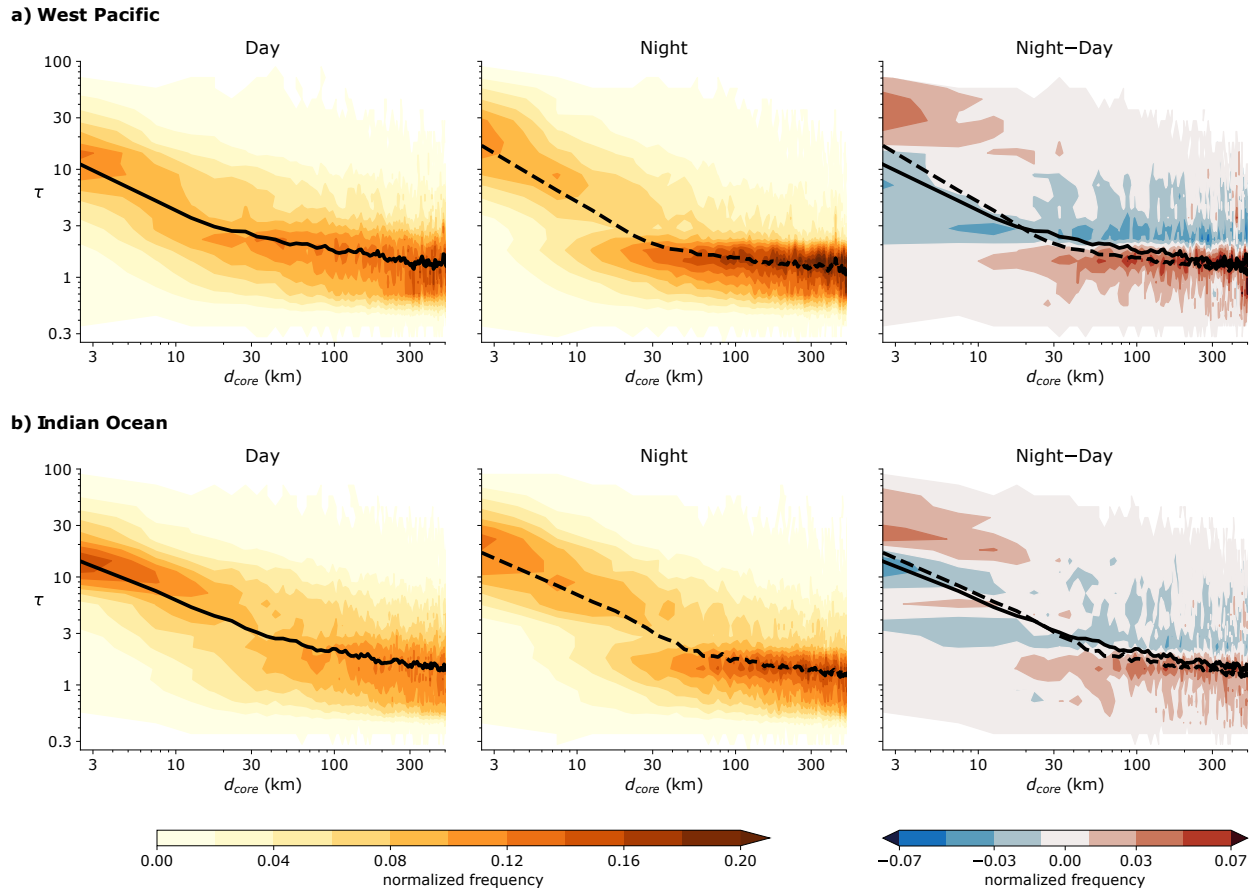
Figure S4. Joint histograms of anvil optical thickness (τ) and spreading distance (d_{core}) for the (a) West Pacific and (b) Indian Ocean regions for (left) day, (middle) night, and (right) night minus day. The histograms are normalized by column so that the sum of all values in each d_{core} bin is 1. Black lines (solid for day, dashed for night) indicate the median τ. Bin widths are 5 km for d_{core} and 0.1 in log space for τ.
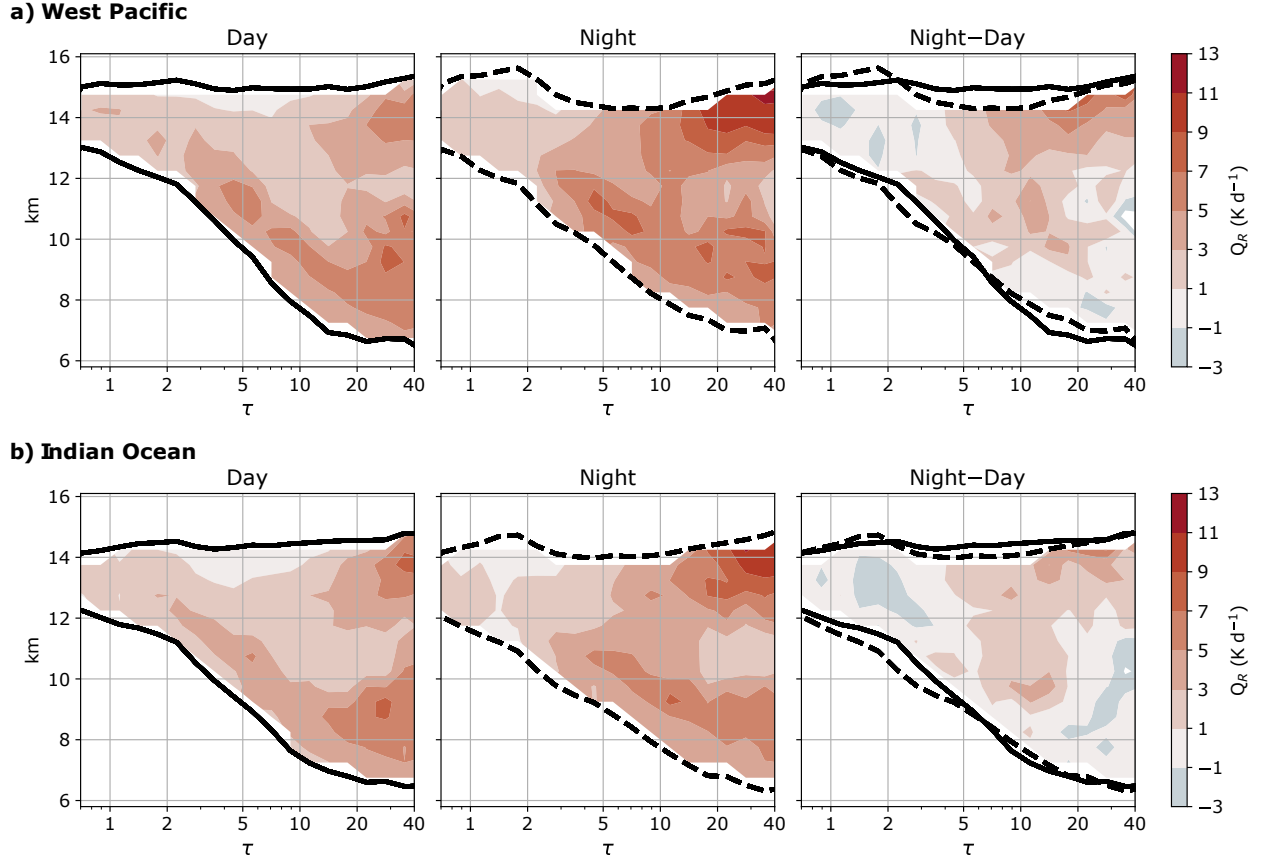
August 27, 2020, 9:57pm

:

Figure S5. Standard deviation of the net radiative heating rates (Q_R) from 100 subsample composites for the (a) West Pacific and (b) Indian Ocean regions for (left) day, (middle) night, and (right) night minus day. Black lines (solid for day, dashed for night) indicate the 100-composite mean cloud top and base heights. The 100 subsample composites are constructed as described in sections 2.3 and 2.4 of the text.
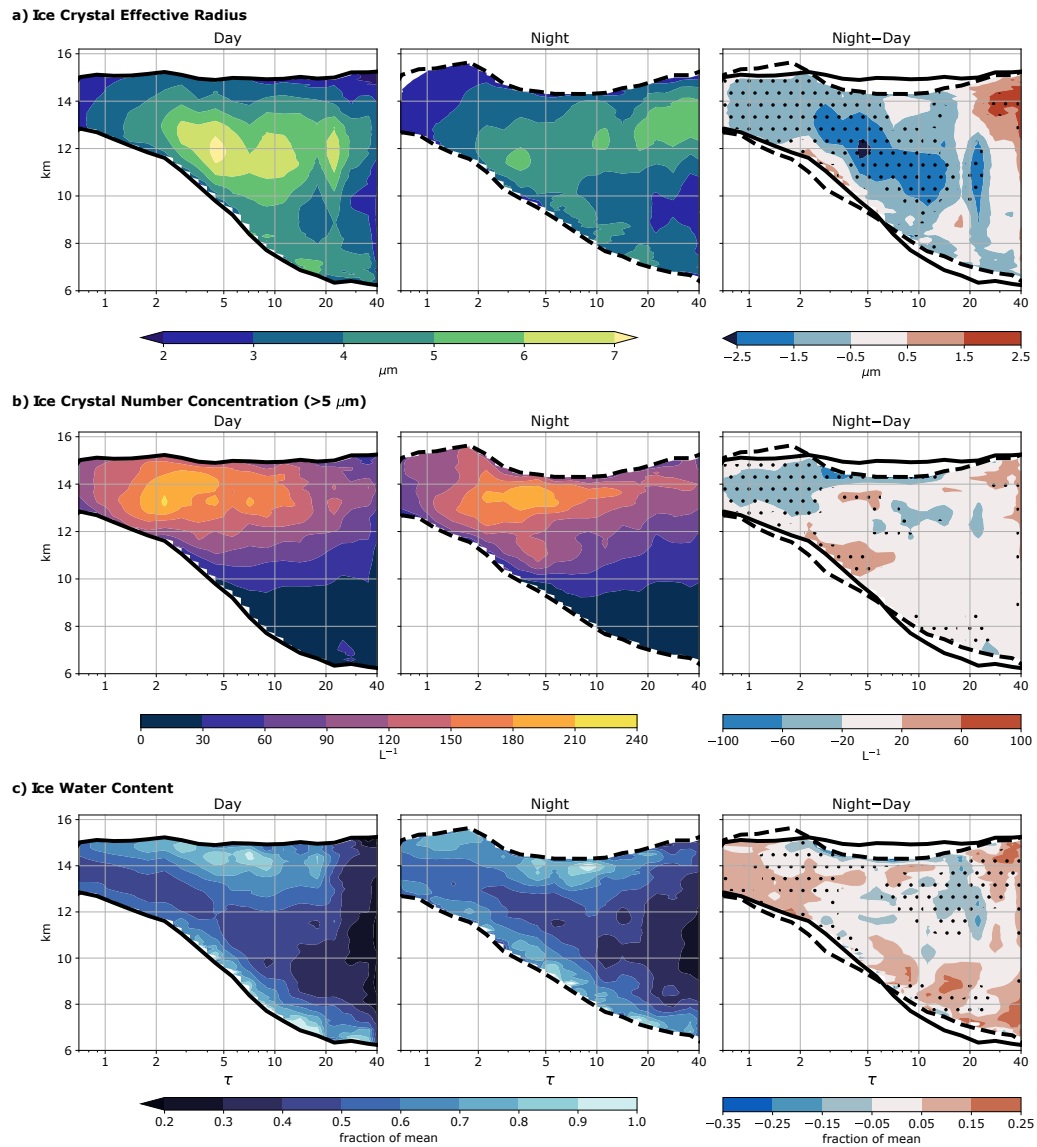
a) Ice Crystal Effective Radius

b) Ice Crystal Number Concentration (>5 μm)

c) Ice Water Content

Figure S6. Standard deviation of (a) effective radius, (b) ice crystal number concentration, and (c) ice water content in the West Pacific for (left) day, (middle) night, and (right) night minus day. For each of the 100 subsample composites, standard deviations are calculated at each altitude level from the individual anvil profiles within each τ bin. The values shown are the averages of the standard deviations from the 100 composites and thus indicate the variability *within* each composite. This differs from Figure S5, which shows variability *among* the 100 composites. Stippling indicates a statistically significant difference between day and night. The standard deviation of IWC is given as a fraction of the 100-composite mean IWC, but statistical significance is calculated based on absolute values. Black lines (solid for day, dashed for night) indicate 100-composite mean cloud top and base heights.
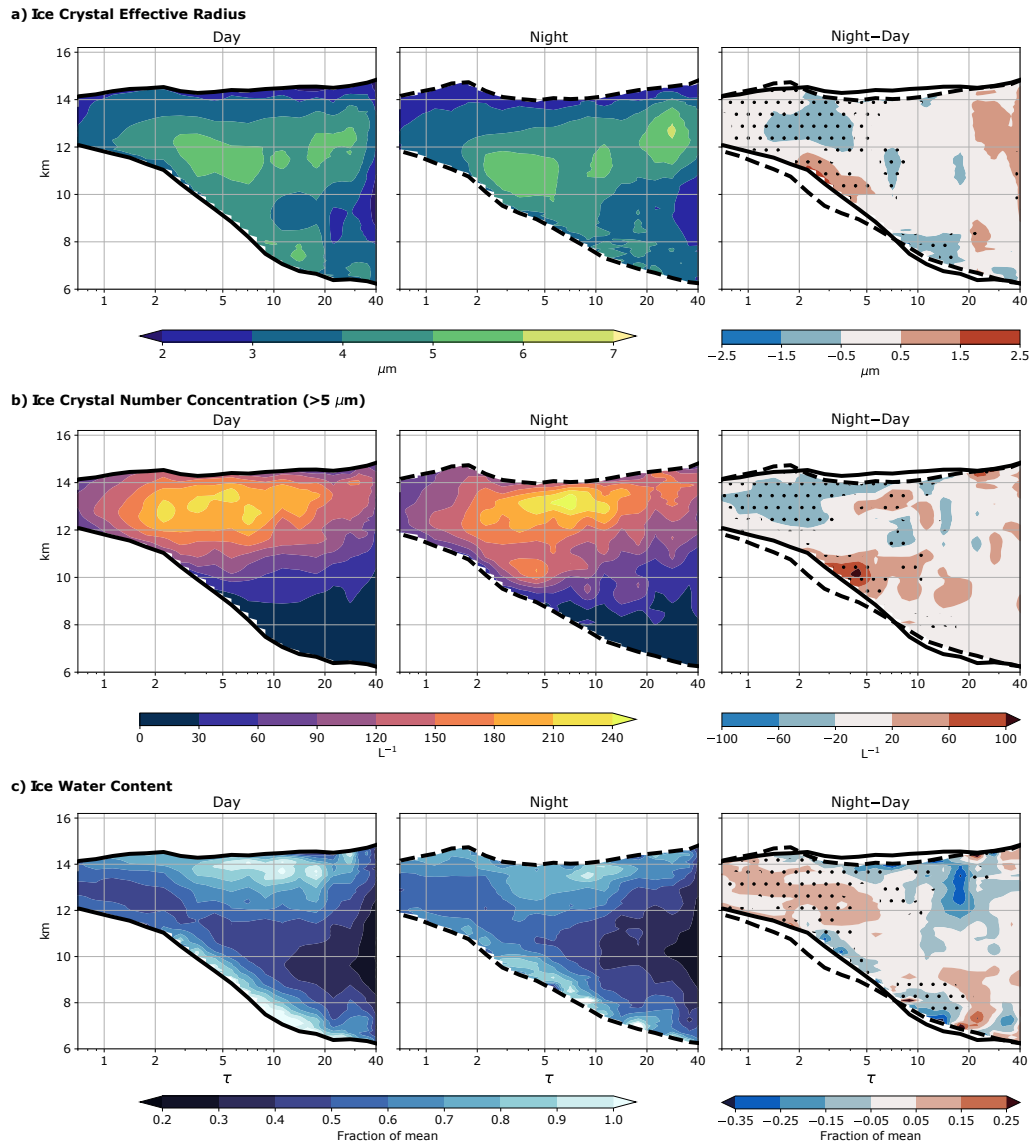
August 27, 2020, 9:57pm

:

a) Ice Crystal Effective Radius

b) Ice Crystal Number Concentration (>5 μm)

c) Ice Water Content

Figure S7. As in Figure S6 but for the Indian Ocean region.

August 27, 2020, 9:57pm